atmosphere

MDPI

Article

Olive and Grass Pollen Concentrations: Evaluation of Forecast Models with Real Observations as Standard in the Évora Region, Portugal

Ana Galveias [1,2,*], Hélder Fraga [3], Ana Rodrigues Costa [1,2] and Célia M. Antunes [1,2]

[1] Department of Medical and Health Sciences, School of Health and Human Development, University of Évora, 7000-67 Évora, Portugal; acrc@uevora.pt (A.R.C.); cmma@uevora.pt (C.M.A.)
[2] CREATE—Center for Sci-Tech Research in Earth System and Energy, University of Évora & Centro Académico Clínico, C-TRAIL, 7000-671 Évora, Portugal
[3] Center for the Research and Technology of Agro-Environmental and Biological Sciencies (CITAB), Institute for Innovation, Capacity Building, and Sustainability of Agri-Food Production (Inov4Agro), University of Trás-os-Montes e Alto Douro (UTAD), P.O. Box 1013, 5000-801 Vila Real, Portugal; hfraga@utad.pt
* Correspondence: acgjorge@uevora.pt

Abstract

Background: The CAMS Regional System provides crucial, reliable pollen forecasts for allergenic pollen types. These robust predictions support the scientific and medical communities, aiding in the diagnosis, evaluation, and protection of allergic populations. So, the main goal of this study was to evaluate which model, or models best represent and simulate the olive and grass pollen data of the Évora region in the years 2021 to 2024. Results: The results showed that there are statistically significant differences between the data of the models and between the years for each of the pollen types considered. These differences were not just in pollen concentrations; they also appeared in characteristics of the pollen season, like its duration, maximum peak concentration, start date and exposure level. According to Taylor diagrams, applying moving average for normalized data, it was shown that MOCAGE best represents and simulates olive concentration data. For grass pollen SILAM, EURAD-IM and MOCAGE were the best performers. Conclusions: CAMS data can enhance the quality of life of the allergic population, as well as support the scientific and medical community to improve, assist and create mitigation measures that reduce exposure and consequently significantly reduce the occurrence of allergic disease.

Keywords: olive pollen; grass pollen; forecast models; observational data

Academic Editor: László Makra

Received: 1 September 2025
Revised: 24 September 2025
Accepted: 27 September 2025
Published: 4 October 2025

Citation: Galveias, A.; Fraga, H.; Costa, A.R.; Antunes, C.M. Olive and Grass Pollen Concentrations: Evaluation of Forecast Models with Real Observations as Standard in the Évora Region, Portugal. *Atmosphere* **2025**, *16*, 1160. https://doi.org/10.3390/atmos16101160

1. Introduction

During the reproduction period, seed plants produce and release biological particles, pollen, into the atmosphere. Pollen is the male gametophyte that contains allergens in its constitution [1]. Anemophilous plants, which rely on wind for pollen dispersal, release large amounts of pollen into the atmosphere, an adaptation to ensure that reproduction is successful. As a result, humans are accidentally exposed to large amounts of pollen, which can cause respiratory problems in susceptible individuals. Upon exposure, susceptible individuals' immune systems recognize pollen allergens as foreign, initiating Type I hypersensitivity reactions, or allergic sensitization [2,3]. Repeated exposure to the allergen may subsequently elicit an allergic response [2,3]. Spring is the peak pollination period for most species, and it is also when most allergic individuals experience symptoms like allergic rhinitis (commonly known as "hay fever" or pollinosis) or, in more severe cases,

allergic asthma [3,4]. The increasing trends of pollen allergies are becoming worrying, and the scientific community has made many efforts to predict pollen concentrations in the air, especially in industrialized countries, this is because the synergy between pollen and air pollution can exacerbate asthma and other allergic manifestations [5,6]. Different studies report that the combined exposure of pollen together with air pollutants, mainly from anthropogenic actions, can amplify allergic disease, increasing the inflammatory response [7,8]. The olive tree is a long-lived tree that humans have cultivated for over 5000 years to obtain products such as olive oil, fruit and wood [9]. It is widely cultivated in the Iberian Peninsula, and there are more than 1500 varieties distributed throughout the world [10]. Despite its considerable socio-economic interest, the olive tree produces pollen that is a leading cause of respiratory allergy, particularly in areas with extensive olive cultivation. The higher incidence of allergy to olive tree pollen occurs during the period of its pollination, May to June [11]. The prevalence of these allergies is influenced by both the concentration of pollen in the air and the length of time individuals are exposed [12,13]. To mitigate pollen-related respiratory allergies, one of the main strategies is to prevent exposure to the allergen. This critically depends on having accurate information or forecasts of daily pollen concentrations [14]. Grass pollen belongs to the Poaceae family, which includes 12,000 species classified in 771 genera, belonging to 12 subfamilies [15]. Most of the species that belong to this family are annual or semi-annual [16], and many of them are important crops such as wheat, rice, corn, oats, rye, barley, etc. In addition to those considered cultivated, wild grasses cover 20% of the earth's surface [16]. The pollination period occurs between April and June, with May being the one with high concentrations, with the wind being the disseminating agent of pollen in the atmosphere. As with olive pollen, the allergic sensitization associated with grass pollen is quite significant and varies from country to country. It is estimated that 20% of the population in Europe has allergic sensitization to this pollen type [17]. Currently, the Copernicus Atmosphere Monitoring Service (CAMS) European air quality forecast service provides observations on the composition of the atmosphere, with the main objective of monitoring air quality, greenhouse gas emissions, aerosol concentrations, and air pollutants [18]. This service provides a multi-model hourly forecast, updated daily and freely available, making CAMS pollen data especially useful for allergy monitoring and alerts. Furthermore, these datasets also provide information about other pollutants that can worsen respiratory symptoms when combined with high pollen concentrations. Recent studies highlight the strong need for accurate predictions and reliable data. This information is crucial, not only as a diagnostic aid for doctors but also for guiding mitigation and protection measures for both the allergic and general populations [19]. The aim of this study is to evaluate existing CAMS service prediction models for daily olive and grass pollen concentrations by comparing them with observational data from the pollen station in the Évora region. To achieve this, data from prediction models between 2021 and 2024 were obtained. The analysis focused on the differences between these models and a comparison of each model with Évora's observational data.

2. Materials and Methods

2.1. Study Area

The Évora region, located in the South of Portugal (38°34′21.5″ N, 7°54′26.45″ W), is characterized as an urban zone. In terms of mainly vegetation, Évora landscape features scrublands, shrubs, pastures and forests dominated by holm oak (*Quercus rotundifólia* L.) and cork oak (*Quercus suber* L.). Olive cultivation is predominant in the Alentejo region, and it recent years, there has been notable increase in planting of olive and almond groves near the city and extending over kilometers. The southernmost area of Évora, approximately

58 km away, has the largest number of olive grove hectares, reaching 74,059 ha (Alqueva Agricultural Yearbook 2024) (www.edia.pt, 25 September 2025). Surrounding the pollen monitoring station, which is part of the Pólen Alert network (https://lince.di.uevora.pt/polen/, 25 September 2025), lies the public garden, where there is higher floral diversity. Species of the Cupressaceae, Sapindaceae, and Taxacecae families, along with several species of the Poaceae family and exotic species, for example, can be found.

2.2. Aerobiological Data

Airborne olive and grass pollen were collected with Hirst-type volumetric spore traps [20] from 2021 to 2024 with a regional representation of >25 km [21]. The sampler was placed at the Évora Atmospheric Sciences Observatory (EVASO), located on the rooftop of the Science and Technology School of the University of Évora (38°34′ N, 7°54′ W) about 10 m above the ground. Slides were analyzed daily under a light microscope (400× magnification), and the results were expressed as pollen per cubic meter of air (Pollen/m^3) according to the European norm EN16868:2019 and [22]. For succinctness, this observational data will be referred to as Data_Station_Evora.

2.3. Model Overview

CAMS is a component of the European Earth observation program, created to design and meet political and scientific needs of interest on environmental issues such as climate change, air pollution, as well as the occurrence of volcanic eruptions. It is a service that provides daily, near-real-time analysis and forecasting of atmospheric composition on a global scale. CAMS also produces a global reanalysis dataset for greenhouse gases and aerosol concentration [23]. CAMS provides several air quality and atmospheric chemistry models. To obtain data on olive and grass pollen concentrations, the CAMS European air quality forecasts were accessed through the Climate Data Store (CDS) API using the libraries. Specifically, we retrieved forecast data from a suite of 12 chemical transport models: CHIMERE, DEHM, EMEP, EURAD-IM, GEM-AQ, LOTOS-EUROS, MATCH (grass pollen not available), MINNI, MOCAGE, MONARCH and SILAM. The data request was restricted to the 00:00 UTC forecast run with a lead time of 0 h, representing the immediate forecast conditions (nowcast), covering the period from 1 January 2021 to 31 December 2024. The data was downloaded in NetCDF format for subsequent processing. A short description of each model is provided below.

2.3.1. CHIMERE

CHIMERE is a multi-scale chemical transport model (CTM) developed by CNRS [22] and further developed by INERIS. It has been in use since the early 2000s [24,25] and is widely used for air quality forecasting in France. CHIMERE operates at spatial resolutions ranging from 100 km to 1 km, from hemispheric to urban scales.

2.3.2. DEHM

DEHM (Danish Eulerian Hemispheric Model) is a large-scale, three-dimensional Eulerian CTM developed in Denmark for studying atmospheric chemical transport in the Northern Hemisphere. Originally developed in the 1990s to study the transport of sulfur compounds in the Arctic [26,27], DEHM continues to be used for long-range pollution studies.

2.3.3. EMEP

EMEP MSC-W is a chemical transport model developed by the Norwegian Meteorological Institute as part of the European Monitoring and Evaluation Programme (EMEP).

Operational since 2006, the model supports studies of chemical mechanisms and aerosol dynamics across Europe.

2.3.4. EURAD-IM

EURAD-IM (European Air Pollution Dispersion—Integrated Model) is a mesoscale Eulerian CTM that processes meteorological data and anthropogenic emissions through CEP and PREP preprocessing systems. It simulates key processes such as advection, diffusion, chemical transformation, deposition, and sedimentation of tropospheric gases and aerosols.

2.3.5. GEM-AQ

GEM-AQ (Global Environmental Multiscale model with Air Quality) is an online coupled meteorology–chemistry model developed at Environment and Climate Change Canada [28]. GEM-AQ integrates air quality components directly into the GEM weather model and is used operationally for air quality forecasting in countries like Poland.

2.3.6. LOTOS-EUROS

(LOng Term Ozone Simulation—EURopean Operational Smog) is a three-dimensional CTM designed to simulate atmospheric pollution in the lower troposphere. It is widely applied in studies of pollutant emissions, particularly nitrogen dioxide (NO_2), ozone (O_3), and particulate matter [29].

2.3.7. MATCH

MATCH (Multi-scale Atmospheric Transport and Chemistry model) is a flexible CTM developed to accommodate various meteorological inputs with different spatial resolutions and projections [30].

2.3.8. MINNI

MINNI (National Integrated Modelling system for air quality in Italy) is an integrated evaluation system used to support air quality policies at national and regional levels. It includes the three-dimensional Eulerian CTM FARM (Flexible Air quality Regional Model), which handles the transport and removal of air pollutants.

2.3.9. MOCAGE

MOCAGE (Modèle de Chimie Atmosphérique à Grande Échelle) is a multiscale 3D CTM developed since the 2000s for both research and operational applications. It supports a wide range of uses including chemical weather forecasting, tracking accidental releases, evaluating transboundary pollution, and assimilating satellite observations.

2.3.10. MONARCH

MONARCH (Multiscale Online Non-hydrostatic AtmospheRe Chemistry model) is an online coupled system for regional and global chemical weather and climate prediction [31,32]. Developed at the Barcelona Supercomputing Center, it integrates meteorological dynamics with gas and aerosol chemistry for high-resolution applications.

2.3.11. SILAM

SILAM (System for Integrated modeLling of Atmospheric composition) is an Eulerian chemical transport model with a transport module based on the [33] advection scheme, modified by [34], and an adaptive vertical diffusion algorithm [35]. SILAM includes a suite of complementary tools such as weather preprocessing, input/output converters, projection, and interpolation routines.

2.4. Main Pollen Seasons

The model data were compared with the observational data from the Évora station (obs). For both datasets, the main pollen season was calculated, determined by the logistic model developed by [36] and modified by [37]. This method is based on fitting a non-linear logistic regression model to the daily accumulated curve for each pollen type [36]. Parameters such as start_date, end_date, SPIn values, Duration Pollen Season (PSD) and *sm.ps* were determined based on asymptotes when pollen amounts are stabilized on the beginning and end of the accumulated curve. The days of low, moderate, high, and very high-risk levels were calculated from the limits imposed by [38] for olive pollen. For grass pollen, the days of low, moderate and high-risk levels were calculated according to the Spanish Aerobiology Network [39].

2.5. Statistical Analysis

Statistical analyses were used to study the relationship between the prediction models' data and pollen data of Évora Station. The data does not follow a normal distribution by Shapiro–Wilk test at a significance level of 5%. Descriptive statistics were used to characterize the data of each model and the data from the pollen station in Évora for the years 2021–2024. Parameters such as mean, median, standard deviation, maximum, and minimum were computed. Due to the high daily variability of pollen data, a 7-day moving average filter was applied to both the observational and modelled datasets, enabling a more accurate comparison of the temporal evolution of pollen levels. Taylor diagrams and scores were plotted to compare the filtered time-series [39]. The Taylor diagram offers a concise way to visualize how well a model agrees with a reference dataset by combining three key statistical measures into a single plot. The correlation coefficient is represented by the angle from the radial distance, indicating how closely the model's pattern follows that of the observations. The vertical axis from the origin corresponds to the model's standard deviation, allowing a direct comparison of variability against the reference. And the horizontal axis is the mean values.

3. Results

3.1. Characterization of Olive and Grass Pollen Season of Évora Station

Marked differences can be observed in pollen levels and pollen season characteristics (start date, duration, peak maximum and exposure level) for both olive and grass pollen across the analyzed years (Figure 1).

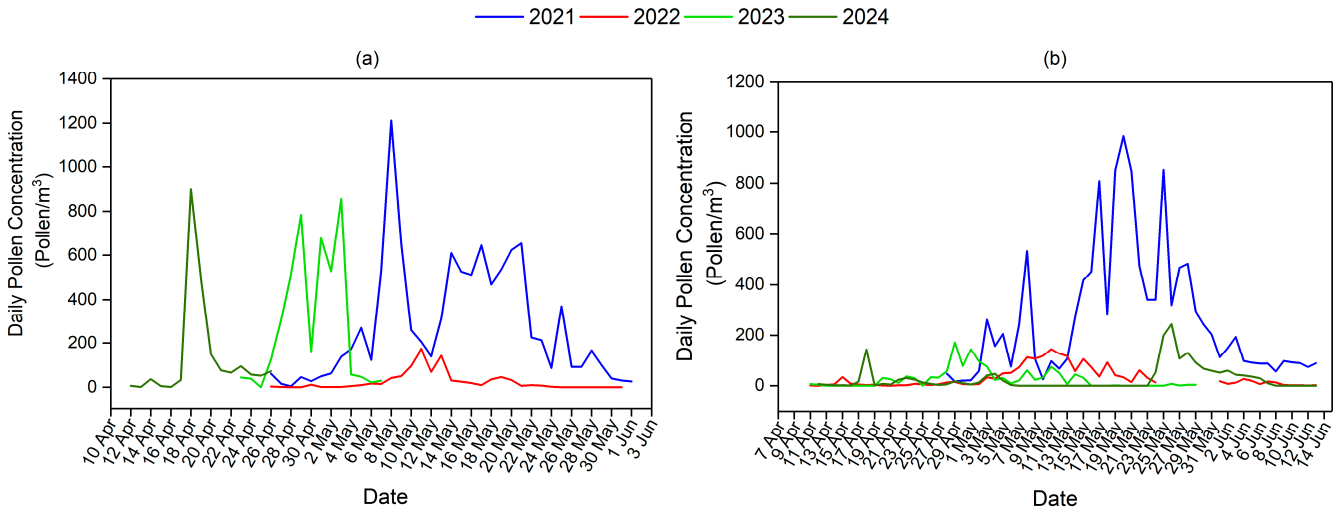

Figure 1. Curve of olive (**a**) and grass (**b**) Main Pollen Season during the years 2021–2024.

Comparing the years, we observed that the main pollen season of the olive pollen season in the region of Évora begins at the end of April, with its end in different periods, as shown in Table 1. However, pollen concentrations, from year to year, were different. The year 2021 recorded the highest pollen concentrations, registering a SPIn value of 10,304 pollen/m^3 compared to 2022, in which a lower SPIn value was obtained (876 pollen/m^3). Regarding the duration of pollen season, for both years, 2021 and 2022, the same duration of the pollen season was observed; however, during the years 2023 and 2024, the duration of the season was significantly lower, with only 15 days. The peak maximum of concentration day was highest in 2021, with 1212 pollen/m^3 compared to the other years. However, in 2024 the peak was recorded earlier, on 18 April (Figure 1 and Table 1).

Table 1. Main pollen season of olive and grass pollen, with parameters such as start date, end date, PSD, SPIn, peak value and peak date determined and represented.

		2021	2022	2023	2024
Olive pollen	Start date	26 April	26 April	23 April	12 April
	End date	01 June	31 May	07 May	26 April
	PSD, number of days	37	36	15	15
	SPIn, pollen/m^3	10,304	876	4198	2055
	Peak value	1212	174	856	900
	Peak date	08 May	11 May	03 May	18 April
	Low (<20 pollen/m^3), number of days	13	18	0	4
	Moderate (20–50 pollen/m^3), number of days	2	6	5	2
	High (51–100 pollen/m^3), number of days	5	3	2	6
	Very high (>101 pollen/m^3), number of days	17	2	8	3
Grass pollen	Start date	28 April	11 April	11 April	12 April
	End date	13 June	15 June	29 May	25 June
	PSD, number of days	47	66	49	75
	SPIn, pollen/m^3	12,282	1890	1242	1787
	Peak value	984	144	171	245
	Peak date	20 May	11 May	29 April	26 May
	Low (1–25 pollen/m^3), number of days	4	32	14	20
	Moderate (26–50 pollen/m^3), number of days	1	9	11	7
	High (>50 pollen/m^3), number of days	42	13	8	11

For grass pollen, the start date was consistent in 2022 and 2023. In 2024 we observed a delay of only one day. We observed that 2021 had higher pollen concentrations compared to the other years, and the peak value followed the same trend, being highest in 2021. However, when looking at the length of the pollen season, 2021 was the year with the lowest number of days, in contrast with 2024, which recorded 75 days (Table 1). Regarding the risk levels, and in the case of olive pollen, the year 2021 presented 17 days of very high risk (>100 pollen/m^3) compared to the other years. Otherwise, the year 2022 was the one with 18 days of low risk (<20 pollen/m^3). The same is observed for grass pollen; the year 2021 had the highest number of high-risk days (42 days) and the year 2022 had the highest number of days with low risk of exposure (32 days) (Table 1).

3.2. Characterization of Olive and Grass Pollen Season of Prediction Models

The different models show high inter-model and inter-year variability (Figures 2–4). Regarding the CHIMERE model, the forecasts of daily pollen concentrations were higher in the year 2024, with a total pollen of 521 pollen/m^3. The main pollen period varied significantly between years, highlighting the 2021 season as exceptionally late, with the peak of maximum concentration on 9 June. In the DEHM model, there is a large discrepancy between the year 2022 and the other years, reaching in this year a peak concentration of 5103 pollen/m^3 on 17 May. For the EMEP model, concentrations reached a maximum value of approximately 8 pollen/m^3 in all years, with 2024 recording the highest concentrations. For the MOCAGE model, 2024 demonstrated the highest pollen concentrations, reaching 2147 pollen/m^3. In contrary, in the years 2022 and 2023, a concentration of less than 200 pollen/m^3 was recorded. In the GEM-AQ model, in 2021 the pollen concentration forecasts only reached 100 pollen/m^3. The years 2022 and 2023 had a very short season duration with concentrations of approximately 800 pollen/m^3. For the MATCH model, only olive pollen data for the years 2021 and 2022 was available. For these years, the highest pollen concentrations were obtained in 2022. For the LOTOS and SILAM models, the year 2023 showed the lowest concentrations. For the MINNI and MONARCH models, data was only available for 2023 and 2024, with the year 2024 consistently showing higher daily pollen forecasts (Figures 2–4 and Table S1).

Regarding grass pollen, between the years 2022 and 2024, it was observed that their minimum variability was at the beginning of the season when comparing the models, except for the MINNI and SILAM models, for which it was not possible to calculate the seasons in the years 2022 and 2023, and the MONARCH model, which showed an early start date of the pollen season (19 February). For the year 2022, the predicted pollen concentrations indicated that the EURAD-IM model had the highest SPIn value (1285 pollen/m^3), while the MONARCH model recorded the lowest SPIn value (5 pollen/m^3) (Table S2). The EMEP model pollen season had the longest duration, with a total of 138 days, followed by the LOTOS-EUROS and CHIMERE models, with 115 and 110 days, respectively, while the shortest season was detected in the MONARCH model, with 36 days. The maximum peak concentration was highest in the EURAD-IM model (146 pollen/m^3), while the EMEP model recorded maximum concentrations of only 1 pollen/m^3 (Figure 4). For 2023, most models indicated the start of the pollination season at the beginning of April. Exceptions were the GEM-AQ and MOCAGE models, for which the start of the season was recorded on 20 May and 27 April, respectively. Regarding SPIn, the EURAD-IM model showed the highest concentration value, with 783 pollen/m^3, followed by the GEM-AQ and MOCAGE models, with 237 and 212 pollen/m^3, respectively. The EMEP model consistently recorded the lowest pollen concentration and the lowest maximum peak concentration (Figures 2–4). For 2024, only the EMEP model showed results; in this model, the pollination season began on 30 April and ended on 30 May, with total concentrations of 40 pollen/m^3. The maximum peak concentration was only 7 pollen/m^3 (Figures 2–4). In general, when we compare the outputs of the models for both pollen types, we observe that pollen concentrations are lower for grass pollen (Figures 2–4 and Table S2).

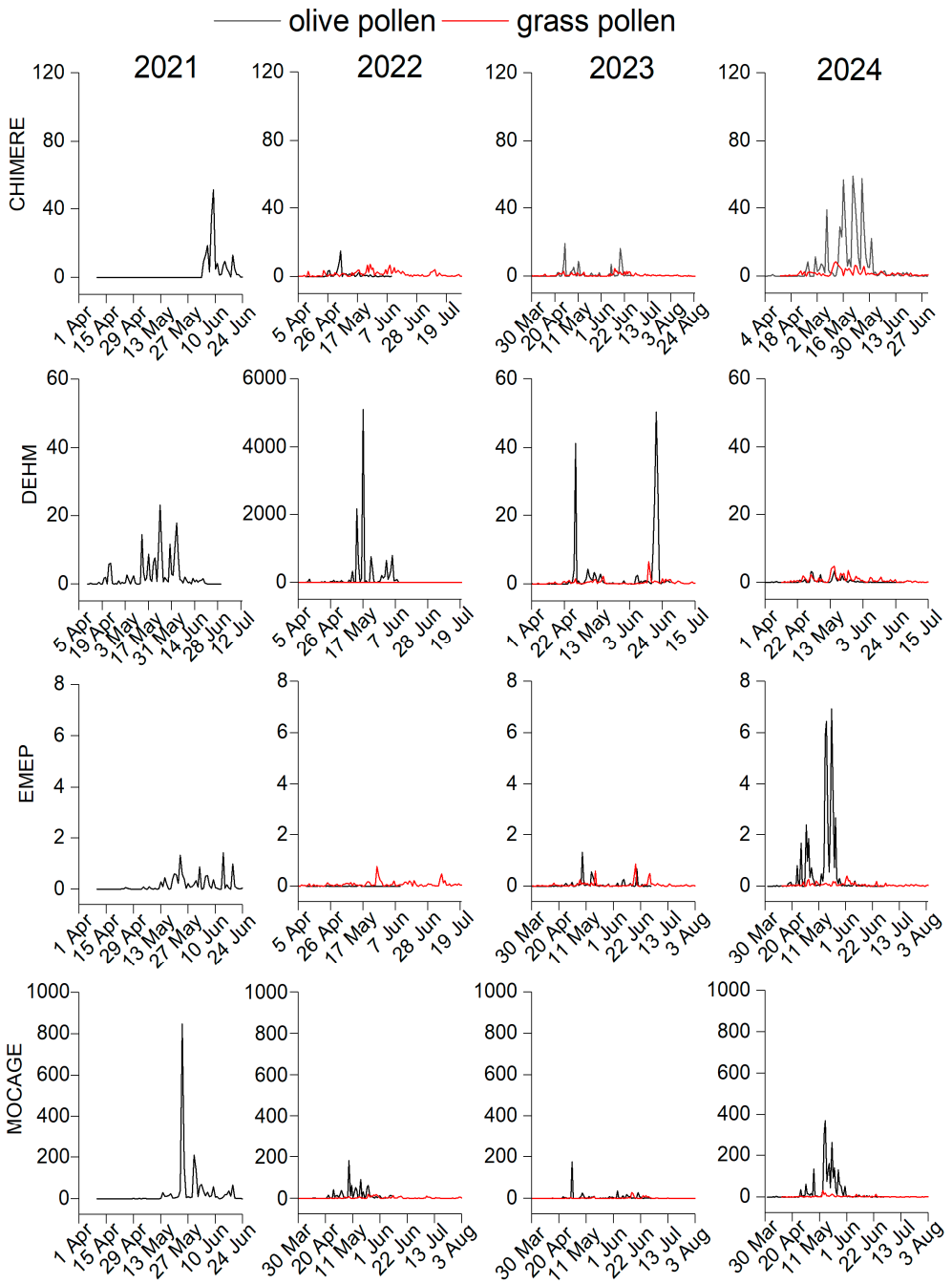

Figure 2. Pollen daily raw timeseries of the CHIMERE, DEHM, EMEP, MOCAGE models.

Regarding olive pollen exposure levels, the MATCH and EMEP models presented only low-risk days in 2021, 45 and 53 days, respectively. For the year 2022, only the EMEP and CHIMERE models had low-risk days, with 68 days and 32 days, respectively. For the year 2023, in addition to those mentioned above, the MINNI model also showed only low-risk days (94 days), and for the year 2024, the EMEP and DEHM models showed 31 and 48 days, respectively (Tables S3–S6). The remaining models, considering all the years under analysis, presented concentrations between low, moderate, high and very high, reaching concentrations above 100 pollen/m^3 (Tables S3–S6).

Considering grass pollen, most models presented only low risk levels, with concentrations between 1 and 25 pollen/m^3. Exceptions were detected in the EURADIM, GEMAQ and MOCAGE models, in which concentrations reached low, moderate and high, with concentrations above 50 pollen/m^3 (Tables S4–S6).

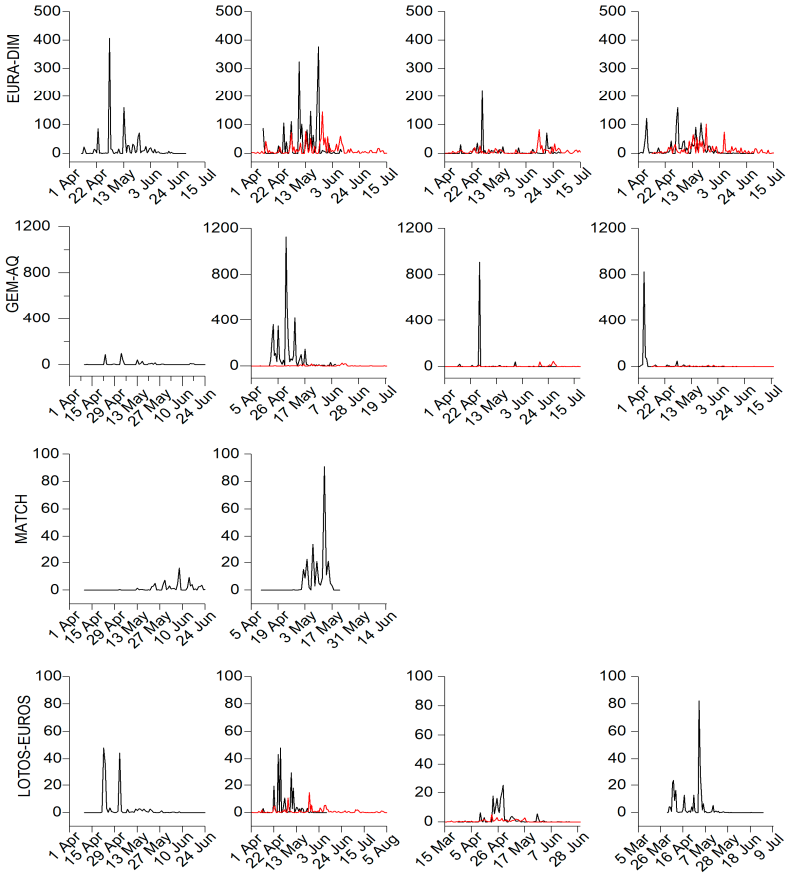

Figure 3. Olive (black line) and grass (red line) pollen daily raw timeseries of the EURAD-IM, GEM-AQ, MATCH, LOTUS models.

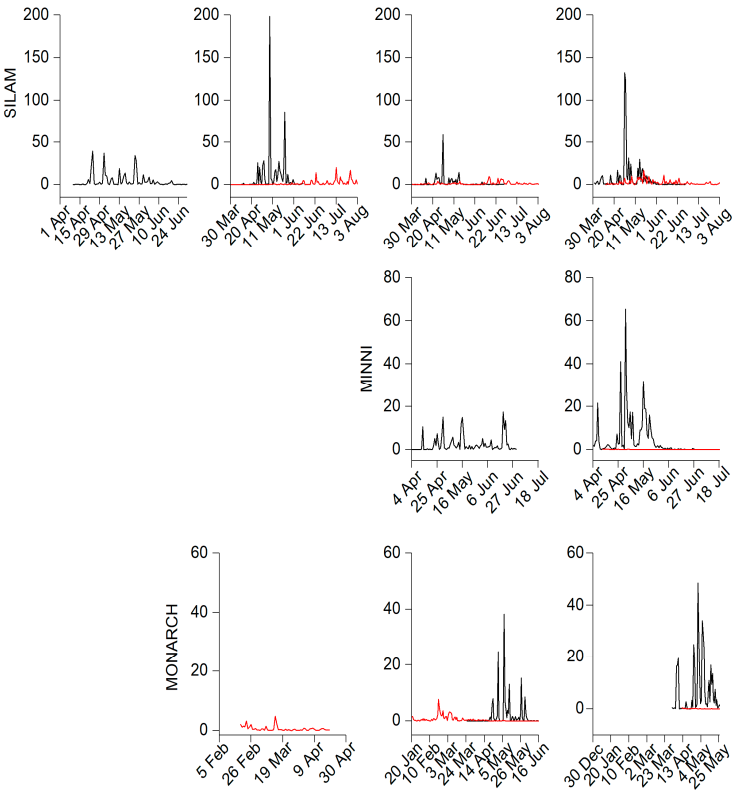

Figure 4. Olive (black line) and grass (red line) pollen daily raw timeseries of the SILAM, MINNI, MONARCH models.

3.3. Comparison Between Pollen Observations and Model Data

In the comparative analysis between the observational data (Data_Evora_Station) and the prediction models selected for this study, it was observed that, depending on the year and pollen type, some models show significant differences not only in the daily pollen concentrations but also in the PSD, peak maximum concentration, start date and end date for both pollen types.

Regarding the comparison of the 7-day moving average filtered timeseries of olive pollen (Figure 5a), model performance is generally weak. Most models exhibit low correlations with observations and underestimate the normalized standard deviation. The best-performing model is MOCAGE, with a score of 0.22, suggesting a modest ability to capture observed variability. Other models, such as CHIMERE, EURAD-IM, and LOTOS-EUROS, follow closely but still show limited skill. At the lower end of the performance spectrum are MINNI and DEHM, which yield near-zero scores and low correlations, indicating poor agreement with observations.

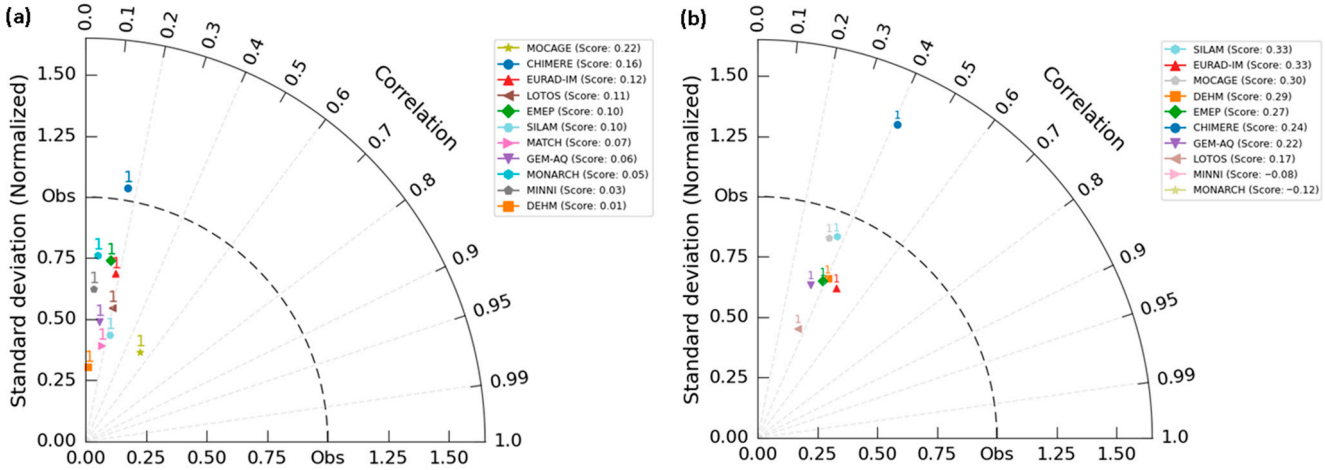

Figure 5. Taylor diagrams depicting model scores compared to the Évora station (Obs) for olive (**a**) and grass (**b**).

In contrast, the performance improves noticeably for grass pollen (Figure 5b). Several models achieve higher correlations and more realistic representations of standard deviation. SILAM and EURAD-IM show the strongest performance, both scoring 0.33, followed closely by MOCAGE and DEHM. These models demonstrate a moderate capacity to replicate the observed seasonal pattern and variability. Conversely, MINNI and MONARCH yield negative scores, reflecting a poor fit to observed data and suggesting potential phase mismatches or over-smoothing. Hence, pollen simulations of grass are more consistent with observations than those of olives. Further, the application of a 7-day moving average highlights the broader temporal trends and facilitates a more robust assessment of model performance.

Regarding PSD (Figure 6) and peak maximum concentration (Figures 7 and 8) between model data and observational data, it was observed that for olive pollen in the year 2021, the duration of the season varied in the models and Data_Station_Evora, between approximately 20 days and 80 days. In Data_Station_Evora the duration of the main pollen season was approximately 40 days, a value that was also observed for MATCH and LOTOS-EUROS. The models that diverged the most were CHIMERE and SILAM. As far as the year 2022 is concerned, the length of the season in Data_Station_Evora was like most models (between 35 and 45 days), with the models that moved the furthest away being EMEP and MATCH (Figure 6a).

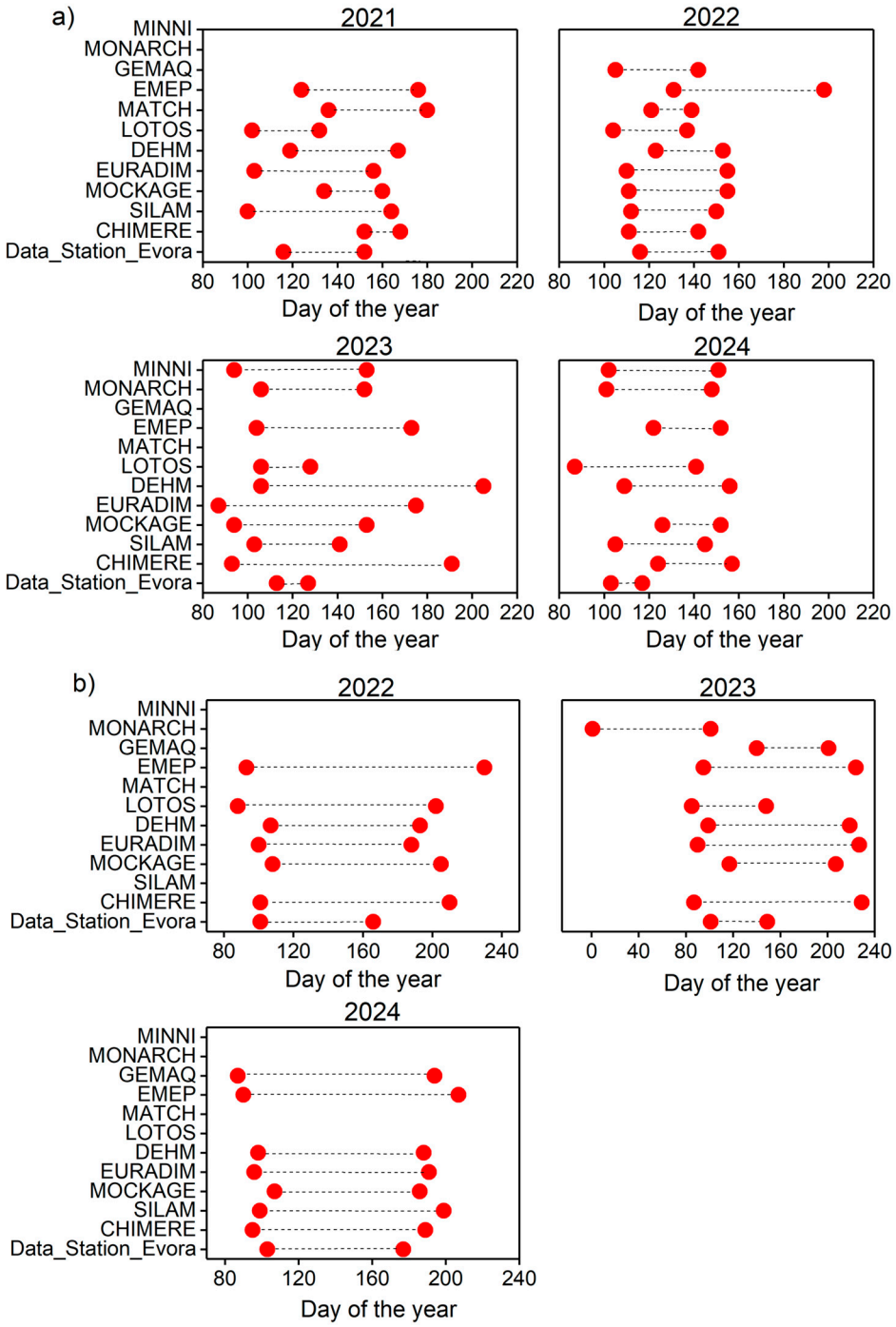

Figure 6. Start-date, end-date and PSD, number of days of models and Data_Station_Evora pollen season. (**a**) Olive pollen season and (**b**) grass pollen season.

In 2023, the pollen season of Data_Station_Evora was particularly short, with a length of 15 days, approaching the LOTOS-EUROS model; however, on the contrary, the EURADIM, DEHM, MINNI, MOCAGE, CHIMERE and EMEP models departed significantly, as they had a season duration of more than 60 days. The season length for Data_Station_Evora in 2024 was like that of 2023; however, the season length for models did not exceed 60 days (Figure 6a). Regarding start date and end date of the pollen season of the prediction models compared to Data_Station_Evora, it was observed that in the year 2021, for olive pollen, the start date of the pollen season occurred between days 100 and 160, with the EMEP and CHIMERE models being the ones that strayed farthest from Data_Station_Evora. The pollen season of the EMEP model started earlier, while it started later for CHIMERE. The MINNI

model was the one that most closely resembled the Data_Station_Evora data. For the year 2022, the times of the models began at about the same period. The model season started later (approximately on the 140th day of the year). As far as the end of the season is concerned, most of the data resembles Data_Station_Evora, except for the EMEP model, which departs significantly. The year 2023 is similar, as well as the start date of the 2022 season. The same is not true for the end date of the season, when there is a great dispersion over a certain period of the year. For the year 2024, the start date of the pollen season calculated from the prediction models showed that the MOCAGE model is the one that moves farther from the beginning of the season of Data_Station_Evora; on the contrary, the SILAM and MINNI models are those that are closest to the period of the beginning of the observational data. Considering the end date of the season, Data_Station_Evora is isolated, and the models LOTOS, SILAM, MONARCH, MINNI, CHIMERE, DEHM, MOCAGE, EURADIM, MATCH and EMEP showed results closer to each other (Figure 6a). Regarding the maximum peak concentration, it was found that in most models and Data_Station_Evora for all years, the maximum peak concentration did not exceed 1200 pollen/m^3, except for the DEHM model for the year 2022, in which the peak concentration was approximately 5000 pollen/m^3. Like Data_Station_Evora in terms of peak maximum concentration, we have the MOCAGE model in 2021 and the GEM-AQ model in 2023 and 2024 (Figure 7).

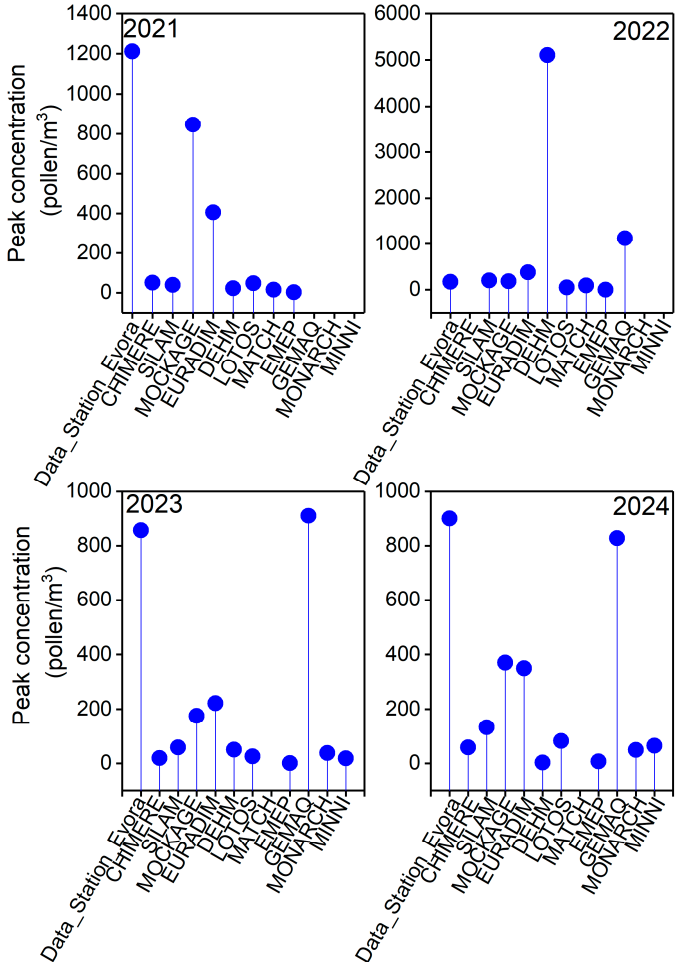

Figure 7. Olive pollen peak maximum of concentration (m^3) at 2021 to 2024.

Regarding grass pollen, it was observed that, in the year 2022, the duration of the season in Data_Station_Evora was 63 days, like the MONARCH model. The CHIMERE and EMEP models were the ones that strayed the furthest from this value. The same pattern

was observed for the year 2023, in which the CHIMERE model had a 140-day pollen season duration and Data_Station_Evora had only 45 days. In both years mentioned above, there is a disparity in the length of the season. For the year 2024, the length of the season is more homogeneous, with the MOCAGE model being the one that comes closest to the calculated season length for Data_Station_Evora and once again the EMEP model to differentiate itself (Figure 6b). Considering start date and end date, the data showed that the start date of the seasons was highly variable over the years. For the year 2021, the start date of the seasons was similar between the models and Data_Station_Evora. The same is not observed at the end of the pollen seasons, in which there was a high temporal dispersion along the established models. For the year 2022, the DEHM model is the one that resembles both the beginning of the season and the end of it. The same occurs for the LOTOS model at the end of the pollen season. The pollen season of the MONARCH model was finished earlier, and the GEM-AQ model showed a later end to the seasons. For the year 2024, the pollen season had an earlier start when compared to the Data_Station_Evora data; however, for the other models there are no significant differences, and, like the observational data, Data_Station_Evora, the pollen season began in the period between days 80 and 110 and ended between days 180 and 210 (Figure 6b).

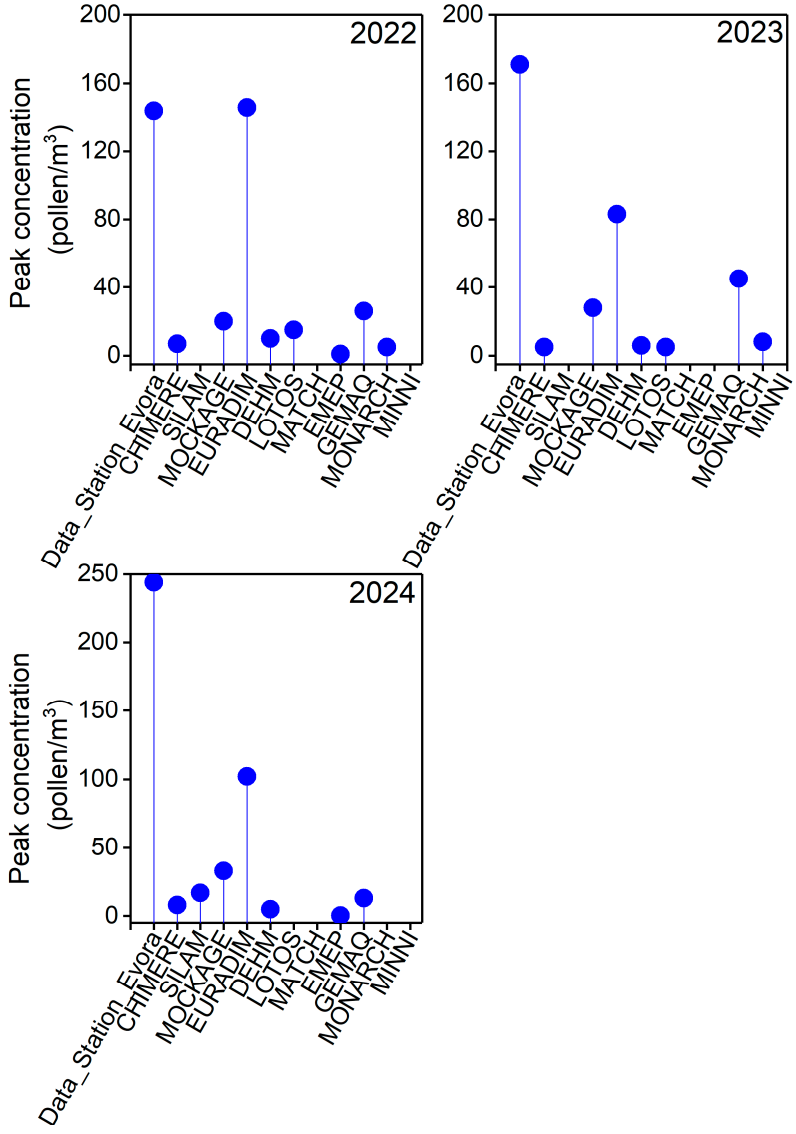

Figure 8. Grass pollen peak maximum of concentration (m^3) at 2022 to 2024.

Regarding the peak maximum concentration, it was observed that, for the year 2022, the peak maximum concentration was 150 pollen/m^3 in the observational data. The same was observed for the EURAD-IM model. Concentrations lower than 50 pollen/m^3 were observed in the EMEP, DEHM, MOCAGE, MONARCH and GEM-AQ models. For the year 2023, the maximum peak concentration for Data_Station_Evora was less than 50 pollen/m^3, the same as observed in the GEM-AQ model. In the year 2024, the peak maximum concentration was significantly different from the models, with a concentration of 250 pollen/m^3 for data of less than 150 pollen/m^3 in the models (Figure 8).

4. Discussion

High concentrations of olive and grass pollen were detected in the atmosphere of Évora during the years 2021–2024 [40]. Our results showed, for olive and grass pollen, differences between the years under study, both in terms of pollen concentrations, duration of pollen season, peak maximum concentration and even the beginning and end of the season. In fact, it is known so far, and although it has not been the subject of this study, that meteorological parameters, particularly temperature and precipitation, have a direct effect on plant phenology with a potential impact on pollen concentrations [17,41–43]. Temperature positively influences daily pollen concentrations and precipitation negatively [41,44]. Regarding the length of the pollen season, it has been found that temperature and precipitation are preponderant factors in determining the period in number of days of the pollen season [43–46]. The same factors are important determinants that influence the beginning of the season [43–46]. The prediction of pollen concentration occurs not only to improve the living conditions of the population, particularly the allergic population, as it allows the allergic population to minimize exposure, but also to alert possible decisions in the field of public health, agriculture and climate change [47]. Prediction models developed to predict airborne pollen concentrations have made significant advances in recent years. Once they have become available to the entire scientific community, with easy access to concentration data, it will be possible to validate them, which contributes to increasing the quality of pollen predictions. To determine which model is most in line with the observational results from our station, a comparison was performed. It is known that the pollen prediction offered by the CAMS service helps in pollen monitoring, and the models that belong to this service present differences in their characteristics and approaches [22]. In fact, each model is different, not only in the input used, but also in the settings or in the data processing method [23–35,48,49]. Daily forecasts are carried out with a spatial resolution of 0.1°, approximately 10–20 km, and each model uses its own data assimilation system. Only the variables related to atmospheric pollutants, such as NO, NO_2, SO_2, O_3 and particulate matter ($PM_{2.5}$, PM_{10} and dust) are regularly validated through in situ observations. Particularly for pollen data, it is possible that, for this reason, discrepancies become pronounced and significant when comparing absolute concentrations between model-generated data and observational data [22,49]. Furthermore, the observational data were obtained using a standardized methodology, in accordance with the European standard [50]. In fact, the MOCAGE model is representative for olive and grass pollen, and the SILAM and EURAD-IM models have been shown to be valid to represent grass pollen concentrations. In addition to the daily pollen concentrations throughout the pollen season, another important parameter is the beginning of the pollen season, not only because it has effects on diagnosis, but also on treatment. In this way, this information is also very useful for forecasting models, to contribute to alerting the population, particularly the allergic population. The ability of each model to predict the beginning of the pollen season can result in significant modeling errors [51], and in addition, the ability of the model to reproduce the beginning of the season varies from year to year. In general, the models

studied for olive and grass pollen show heterogeneity when we consider the beginning and end of the pollen season, compared to the observational data, since there are models starting the season earlier and others later. In fact, studies have been carried out to calibrate prediction models, i.e., it has been shown that the specific pollen types evaluated by models, and compared with observational data from several stations, showed a difference of days compared with the observation data (taken as control). Location is also an important factor [52]. The beginning of the season occurred earlier when considering the regions of Western Europe compared with regions of Southern Europe and Northern Europe [49,52]. The prediction of pollen concentrations and the specific parameters of pollen seasons for each pollen type are important information with direct implications in several sectors of activity, not only around public health, but also in agriculture and climate change. The relevance of pollen prediction, creation of prediction models or even the tuning of existing models has been a concern in recent years, since the increase in the occurrence of respiratory allergic diseases has been notorious, particularly in a context of climate change, which can change the pattern of distribution and dissemination of pollen, significantly affecting the allergic population [14].

5. Conclusions

CAMS data can improve the quality of life of the allergic population, as well as support the scientific and medical community to improve, assist and create mitigation measures that reduce exposure and consequently significantly reduce the occurrence of allergic disease. The results presented in this study contribute significantly to an evaluation of the quality of the predictions of the CAMS models for the region of Évora. However, when we analyze and compare the predictions of the CAMS models with the observational data of the station, we find that there are specific models that approximate the observational data of the station for pollen concentrations: the MOCAGE model for olive pollen, and the EURAD-IM, SILAM and MOCAGE models for grass pollen. For the other characteristics of the seasons, such as the duration, beginning and end and even peak maximum concentration, there is a lot of disparity. In any case, we can say that the MOCAGE model is the most suitable for predicting pollen concentrations for the region of Évora and thus enables a better response for the population.

Supplementary Materials: The following supporting information can be downloaded at: https://www.mdpi.com/article/10.3390/atmos16101160/s1, Table S1: Descriptive characterization of olive pollen concentrations of models between 2021 to 2024; Table S2: Descriptive characterization of grass pollen concentrations of models between 2022 to 2024; Table S3: 2021 Exposure risk levels (in days) for olive pollen; Table S4: 2022 Exposure risk levels (in days) for olive and grass pollen; Table S5: 2023 Exposure risk levels (in days) for olive and grass pollen and Table S6: 2024 Exposure risk levels (in days) for olive and grass pollen.

Author Contributions: All the authors actively and significantly contributed to this manuscript, as follows: Conceptualization, A.G. and H.F.; methodology, A.G. and H.F.; validation, A.G. and H.F.; formal analysis, A.G. and H.F.; investigation, A.G.; resources, C.M.A. and A.R.C.; data curation, A.G. and H.F.; writing—original draft preparation, A.G., A.R.C. and H.F.; writing—review and editing, C.M.A. and A.R.C.; visualization, A.G., A.R.C., C.M.A. and H.F. supervision, C.M.A.; project administration, C.M.A. and A.R.C.; funding acquisition, A.R.C., C.M.A. and H.F. All authors have read and agreed to the published version of the manuscript.

Funding: The work is funded by national funds through FCT—Fundação para a Ciência e Tecnologia, I.P., in the framework of the UID/06107/2023—Centro de Investigação em Ciência e Tecnologia para o Sistema Terra e Energia (CREATE).

Institutional Review Board Statement: Not applicable.

Informed Consent Statement: Not applicable.

Data Availability Statement: Publicly available datasets of meteorological data were analyzed in this study. Pollen datasets are accessible either at [https://lince.di.uevora.pt/polen/index.jsp, 13 January 2025] upon request or within this article.

Acknowledgments: The authors gratefully acknowledge the CAMS, Copernicus Atmosphere Monitoring Service, that provides information of daily pollen data for each model.

Conflicts of Interest: The authors declare no conflicts of interest.

References

1. William. The Male Gametophyte Enclosed in a Pollen Wall. In *Conifer Reproductive Biology*; Springer: Dordrecht, The Netherlands, 2009. [CrossRef]
2. D'Amato, G.; Cecchi, L.; Bonini, S.; Nunes, C.; Annesi-Maesano, I.; Behrendt, H.; Liccardi, G.; Popov, T.; van Cauwenberge, P. Allergenic pollen and pollen allergy in Europe. *Allergy* **2007**, *62*, 976–990. [CrossRef] [PubMed]
3. Erbas, B.; Akram, M.; Dharmage, S.C.; Tham, R.; Dennekamp, M.; Newbigin, E.; Taylor, P.; Tang, M.L.; Abramson, M.J. The role of seasonal grass pollen on childhood asthma emergency department presentations. *Clin. Exp. Allergy* **2012**, *42*, 799–805. [CrossRef] [PubMed]
4. D'AMato, G.; Spieksma, F.T.M. Allergenic pollen in europe. *Grana* **1991**, *30*, 67–70. [CrossRef]
5. D'Amato, G.; Bergmann, K.C.; Cecchi, L.; Annesi-Maesano, I.; Sanduzzi, A.; Liccardi, G.; Vitale, C.; Stanziola, A.; D'Amato, M. Climate change and air pollution: Effects on pollen allergy and other allergic respiratory diseases. *Allergo. J. Int.* **2014**, *23*, 17–23. [CrossRef] [PubMed Central]
6. Gleason, J.A.; Bielory, L.; Fagliano, J.A. Associations between ozone, PM2. 5, and four pollen types on emergency department pediatric asthma events during the warm season in New Jersey: A case-crossover study. *Environ. Res.* **2014**, *132*, 421–429. [CrossRef]
7. Zhang, R.; Duhl, T.; Salam, M.T.; House, J.M.; Flagan, R.C.; Avol, E.L.; Gilliland, F.D.; Guenther, A.; Chung, S.H.; Lamb, B.K.; et al. Development of a regional-scale pollen emission and transport modeling framework for investigating the impact of climate change on allergic airway disease. *Biogeosciences* **2013**, *10*, 3977–4023. [CrossRef] [PubMed]
8. Li, C.H.; Sayeau, K.; Ellis, A.K. Air Pollution and Allergic Rhinitis: Role in Symptom Exacerbation and Strategies for Management. *J. Asthma Allergy* **2020**, *13*, 285–292. [CrossRef] [PubMed] [PubMed Central]
9. Rallo, L. Olive Cultivars in Spain. *HortTechnology* **2000**, *10*, 107–110. [CrossRef]
10. Bartolini, G.; Prevost, G.; Messeri, C.; Carignani, G. (Eds.) *Olive Germplasm: Cultivars and World-Wide Collections*; FAO: Rome, Italy, 1998.
11. Pólen Alert. 2005. Available online: https://lince.di.uevora.pt/polen/ (accessed on 19 March 2025).
12. Tejera, M.L.; Villalba, M.; Batanero, E.; Rodríguez, R. Identification, isolation, and characterization of Ole e 7, a new allergen of olive tree pollen (1999). *J. Allergy Clin. Immunol.* **1999**, *104*, 797–802. [CrossRef] [PubMed]
13. Baldo, R.C.; Panzani, D.; Bass, R. Zerboni. *Mol. Immunol.* **1991**, *29*, 1209–1218. [CrossRef]
14. Oh, J.-W. Pollen Allergy in a Changing Planetary Environment. *Allergy Asthma Immunol. Res.* **2022**, *14*, 168–181. [CrossRef]
15. Soreng, R.J.; Peterson, P.M.; Romaschenko, K.; Davidse, G.; Zuloaga, F.O.; Judziewicz, E.J.; Filgueiras, T.S.; Davis, J.I.; Morrone, O. A worldwide phylogenetic classification of the Poaceae (*Gramineae*). *J. Syst. Evol.* **2015**, *53*, 117–137. [CrossRef]
16. Watson, L.; Dallwitz, M.J. The Grass Genera of the World: Descriptions, Illustrations, Identification, and Information Retrieval; Including Synonyms, Morphology, Anatomy, Physiology, Phytochemistry, Cytology, Classification, Pathogens, World and Local Distribution, and References. 1992. Available online: https://www.delta-intkey.com/grass/index.htm (accessed on 10 May 2025).
17. Rodríguez-Rajo, F.J.; Fdez-Sevilla, D.; Stach, A.; Jato, V. Assessment between pollen seasons in areas with different urbanization level related to local vegetation sources and differences in allergen exposure. *Aerobiologia* **2010**, *26*, 1–14. [CrossRef]
18. Peuch, V.-H.; Engelen, R.; Rixen, M.; Dee, D.; Flemming, J.; Suttie, M.; Ades, M.; Agustí-Panareda, A.; Ananasso, C.; Andersson, E.; et al. The Copernicus Atmosphere Monitoring Service: From Research to Operations. *Bull. Amer. Meteor. Soc.* **2022**, *103*, E2650–E2668. [CrossRef]
19. Suanno, C.; Aloisi, I.; Fernández-González, D.; Duca, S. Pollen forecasting and its relevance in pollen allergen avoidance. *Environ. Res.* **2021**, *200*, 111150. [CrossRef] [PubMed]
20. Hirst, J.M. An Automatic Volumetric Spore Trap. *Ann. Appl. Biol.* **1952**, *39*, 257–265. [CrossRef]
21. Oteros, J.; Sofiev, M.; Smith, M.; Clot, B.; Damialis, A.; Prank, M.; Werchan, M.; Wachter, R.; Weber, A.; Kutzora, S.; et al. Building an automatic pollen monitoring network (ePIN): Selection of optimal sites by clustering pollen stations. *Sci. Total. Environ.* **2019**, *688*, 1263–1274. [CrossRef] [PubMed]

22. Copernicus Atmosphere Monitoring Service (2021): CAMS European Air Quality Reanalyses. Copernicus Atmosphere Monitoring Service (CAMS) Atmosphere Data Store. Available online: https://doi.org/10.24381/7cc0465a (accessed on 24 September 2025).
23. Galan, C.; Smith, M.; Thibaudon, M.; Frenguelli, G.; Oteros, J.; Gehrig, R.; Berger, U.E.; Clot, B.; Brandao, R. Pollen monitoring: Minimum requirements and reproducibility of analysis. *Aerobiologia* **2014**, *30*, 385–395. [CrossRef]
24. Wagner, A.; Bennouna, Y.; Blechschmidt, A.-M.; Brasseur, G.; Chabrillat, S.; Christophe, Y.; Errera, Q.; Eskes, H.; Flemming, J.; Hansen, K.M.; et al. Comprehensive evaluation of the Copernicus Atmosphere Monitoring Service (CAMS) reanalysis against independent observations: Reactive gases. *Elem. Sci. Anthr.* **2021**, *9*, 171. [CrossRef]
25. Mailler, S.; Menut, L.; Khvorostyanov, D.; Valari, M.; Couvidat, F.; Siour, G.; Turquety, S.; Briant, R.; Tuccella, P.; Bessagnet, B.; et al. CHIMERE-2017: From urban to hemispheric chemistry-transport modeling. *Geosci. Model Dev.* **2017**, *10*, 2397–2423. [CrossRef]
26. Bessagnet, B.; Hodzic, A.; Vautard, R.; Beekmann, M.; Cheinet, S.; Honoré, C.; Liousse, C.; Rouil, L. Aerosol modeling with CHIMERE—Preliminary evaluation at the continental scale. *Atmos. Environ.* **2004**, *38*, 2803–2817. [CrossRef]
27. Christensen, J.H.; Brandt, J.; Frohn, L.M.; Skov, H. Modelling of Mercury in the Arctic with the Danish Eulerian Hemispheric Model. *Atmos. Chem. Phys.* **2004**, *4*, 2251–2257. [CrossRef]
28. Heidam, N.; Christensen, J.; Wåhlin, P.; Skov, H. Arctic atmospheric contaminants in NE Greenland: Levels, variations, origins, transport, transformations and trends 1990–2001. *Sci. Total Environ.* **2004**, *331*, 5–28. [CrossRef]
29. Kaminski, J.W.; Neary, L.; Struzewska, J.; McConnell, J.C.; Lupu, A.; Jarosz, J.; Toyota, K.; Gong, S.L.; Côté, J.; Liu, X.; et al. GEM-AQ, an on-line global multiscale chemical weather modelling system: Model description and evaluation of gas phase chemistry processes. *Atmos. Chem. Phys.* **2008**, *8*, 3255–3281. [CrossRef]
30. Hendriks, C.; Forsell, N.; Kiesewetter, G.; Schaap, M.; Schöpp, W. Ozone concentrations and damage for realistic future European climate and air quality scenarios. *Atmos. Environ.* **2016**, *144*, 208–219. [CrossRef]
31. Robertson, L.; Langner, J.; Engardt, M. An Eulerian Limited-Area Atmospheric Transport Model. *J. Appl. Meteor. Climatol.* **1999**, *38*, 190–210. [CrossRef]
32. Badia, A.; Jorba, O.; Voulgarakis, A.; Dabdub, D.; García-Pando, C.P.; Hilboll, A.; Gonçalves, M.; Janjic, Z. Description and evaluation of the Multiscale Online Nonhydrostatic AtmospheRe CHemistry model (NMMB-MONARCH) version 1.0: Gas-phase chemistry at global scale. *Geosci. Model Dev.* **2004**, *10*, 609–638. [CrossRef]
33. Di Tomaso, E.; Escribano, J.; Basart, S.; Ginoux, P.; Macchia, F.; Barnaba, F.; Benincasa, F.; Bretonnière, P.-A.; Buñuel, A.; Castrillo, M.; et al. The Monarch high-resolution reanalysis of desert dust aerosol over Northern Africa, the Middle East and Europe (2007–2016). *Earth Syst. Sci. Data* **2022**, *14*, 2785–2816. [CrossRef]
34. Galperin, M.V. The Approaches to Correct Computation of Airborne Pollution Advection. In *Problems of Ecological Monitoring and Ecosystem Modelling*; XVII; Gidrometeoizdat: St. Petersburg, Russia, 2000; pp. 54–68.
35. Sofiev, M.; Vira, J.; Kouznetsov, R.; Prank, M.; Soares, J.; Genikhovich, E. Construction of the SILAM Eulerian atmospheric dispersion model based on the advection algorithm of Michael Galperin. *Geosci. Model Dev.* **2015**, *8*, 3497–3522. [CrossRef]
36. Sofiev, M.; Sofieva, S.; Palamarchuk, J.; Šaulienė, I.; Kadantsev, E.; Atanasova, N.; Fatahi, Y.; Kouznetsov, R.; Kuula, J.; Noreikaite, A.; et al. Bioaerosols in the atmosphere at two sites in Northern Europe in spring 2021: Outline of an experimental campaign. *Environ. Res.* **2022**, *214*, 113798. [CrossRef]
37. Ribeiro, H.; Abreu, I. A 10-year survey of allergenic airborne pollen in the city of Porto (Portugal). *Aerobiologia* **2014**, *30*, 333–334. [CrossRef]
38. Cunha, M.; Ribeiro, H.; Costa, P.; Abreu, I. A comparative study of vineyard phenology and pollen metrics extracted from airborne pollen time series. *Aerobiologia* **2015**, *31*, 45–56. [CrossRef]
39. Viney, A.; Nicolás, J.F.; Galindo, N.; Fernández, J.; Soriano-Gomis, V.; Varea, M. Assessment of the external contribution to Olea pollen levels in southeastern Spain. *Atmos. Environ.* **2021**, *257*, 118481. [CrossRef]
40. REA. 2025. Available online: https://www.uco.es/rea/ (accessed on 17 July 2025).
41. Zar, J.H. *Biostatistical Analysis*, 5th ed.; Prentice Hall: Upper Saddle River, NJ, USA, 2007.
42. Sabariego, S.; Cuesta, P.; Fernández-González, F.; Pérez-Badia, R. Models for forecasting airborne Cupressaceae pollen levels in central Spain. *Int. J. Biometeorol.* **2012**, *56*, 253–258. [CrossRef]
43. Galveias, A.; Costa, A.R.; Bortoli, D.; Alpizar-Jara, R.; Salgado, R.; Costa, M.J.; Antunes, C.M. Cupressaceae Pollen in the City of Évora, South of Portugal: Disruption of the Pollen during Air Transport Facilitates Allergen Exposure. *Forests* **2021**, *12*, 64. [CrossRef]
44. Galveias, A.; Duarte, E.; Raposo, M.; Costa, M.J.; Costa, A.R.; Antunes, C.M. Trends in land cover and in pollen concentration of Quercus genus in Alentejo, Portugal: Effects of climate change and health impacts. *Environ. Pollut.* **2024**, *362*, 124996. [CrossRef]
45. Schramm, P.J.; Brown, C.L.; Saha, S.; Conlon, K.C.; Manangan, A.P.; Bell, J.E.; Hess, J.J. A systematic review of the effects of temperature and precipitation on pollen concentrations and season timing, and implications for human health. *Int. J. Biometeorol.* **2021**, *65*, 1615–1628. [CrossRef] [PubMed] [PubMed Central]
46. Vázquez, L.M.; Galán, C.; Domínguez-Vilches, E. Influence of meteorological parameters on olea pollen concentrations in Córdoba (South-western Spain). *Int. J. Biometeorol.* **2003**, *48*, 83–90. [CrossRef] [PubMed]

47. Tummon, F.; Bruffaerts, N.; Celenk, S.; Choël, M.; Clot, B.; Crouzy, B.; Galán, C.; Gilge, S.; Hajkova, L.; Mokin, V.; et al. Towards standardisation of automatic pollen and fungal spore monitoring: Best practises and guidelines. *Aerobiologia* **2022**, *40*, 39–55. [CrossRef]
48. Menut, L.; Siour, G.; Mailler, S.; Couvidat, F.; Bessagnet, B. Observations and regional modeling of aerosol optical properties, speciation and size distribution over Northern Africa and western Europe. *Atmos. Chem. Phys.* **2016**, *16*, 12961–12982. [CrossRef]
49. Adamov, S.; Pauling, A. A real-time calibration method for the numerical pollen forecast model COSMO-ART. *Aerobiologia* **2023**, *39*, 327–344. [CrossRef]
50. *EN 16868:2019*; Ambient Air-Sampling and Analysis of Airborne Pollen Grains and Fungal Spores for Networks Related to Allergy-Volumetric Hirst Method CEN, Brussels. German Institute for Standardisation: Berlin, Germany, 2019. Available online: https://standards.iteh.ai/catalog/standards/cen/5f1349aa-f4cc-430a-978e-3044737e3f28/en-16868-2019 (accessed on 25 January 2025).
51. Myszkowska, D. Predicting tree pollen season start dates using thermal conditions. *Aerobiologia* **2014**, *30*, 307–321. [CrossRef] [PubMed] [PubMed Central]
52. Boreczek, J.; Werner, M.; Kryza, M.; Malkiewicz, M.; Benedictow, A.; Chłopek, K.; Dąbrowska-Zapart, K.; Grewling, Ł.; Lipiec, A.; Kalinowska, E.; et al. Modelling of airborne birch pollen over Central Europe—Model evaluation and sensitivity analysis. *Sci. Total. Environ.* **2025**, *990*, 179873. [CrossRef] [PubMed]